JACS
JOURNAL OF THE AMERICAN CHEMICAL SOCIETY

Communication

pubs.acs.org/JACS

Photoinduced Electron Transfer of DNA/Ag Nanoclusters Modulated by G-Quadruplex/Hemin Complex for the Construction of Versatile Biosensors

Libing Zhang, Jinbo Zhu, Shaojun Guo, Tao Li, Jing Li, and Erkang Wang*

State Key Laboratory of Electroanalytical Chemistry, Changchun Institute of Applied Chemistry, Chinese Academy of Sciences, Changchun 130022, China, and University of the Chinese Academy of Sciences, Beijing 100039, China

Supporting Information

ABSTRACT: Photoinduced electron transfer (PET) has been observed for the first time between DNA/Ag fluorescent nanoclusters (NCs) and G-quadruplex/hemin complexes, accompanied by a decrease in the fluorescence of the DNA/Ag NCs. In this PET process, a parallel G-quadruplex and the sensing sequences are blocked by a duplex. The specific combination of targets with the sensing sequence triggers the release of the G-quadruplex and allows it to fold properly and bind hemin to form a stable G-quadruplex/hemin complex. The complex proves favorable for PET because it makes the G-quadruplex bind hemin tightly, which promotes the electron transfer from the DNA/Ag NCs to the hemin Fe^{III} center, thus resulting in a decrease in the fluorescence intensity of the DNA/Ag NCs. This novel PET system enables the specific and versatile detection of target biomolecules such as DNA and ATP with high sensitivity based on the choices of different target sequences.

Molecular beacons (MBs), hairpin-shaped nucleic acid probes that fluoresce upon hybridization with specific nucleic acid targets, have been widely used in biological assays.[1] However, conventional MBs usually require labeling with an appropriate fluorescent dye/quencher,[2] resulting in not only a high cost of operation but also potentially complex processes. Moreover, their low quenching efficiency also limits the assay sensitivity.[3] To obtain enhanced quenching efficiency while simplifying the operation process, it is of great interest to search for new low-cost donor−acceptor pairs as sensing platforms for analytical applications. Recently, silver nanoclusters stabilized by oligonucleotides (DNA/Ag NCs), which exhibit strong, robust, and size-dependent fluorescence emission, have been developed as a new class of fluorophores[4] that have been successfully applied for the detection of various biologically important analytes based on different signal-transducing mechanisms.[5] For instance, it was found that DNA/Ag NCs can act as an interesting fluorescent probe for discriminating a typical single-nucleotide mutation, taking advantage of their strong dependence on the sequence of the DNA scaffold or their emission of distinct colors through interactions with different enhancer sequences.[6] However, the scarcity of efficient and accurate approaches for modulating the fluorescence of DNA/Ag NCs restricts their potential for general application in complex biological and environmental analysis.

Herein we demonstrate a new proof-of-concept that photoinduced electron transfer (PET) between DNA/Ag NCs and G-quadruplex/hemin complexes, accompanied by a decrease in the fluorescence of DNA/Ag NCs (Scheme 1A), can be used to develop a nanocluster-based molecular beacon (NMB) for the detection of target biomolecules with high selectivity and sensitivity. In this PET process, the formed DNA/Ag NCs display strong fluorescence, whereas the G-rich DNA sequence can fold into a G-quadruplex structure. When hemin is introduced, the G-quadruplex/hemin complex is formed and acts as the electron acceptor. PET from the DNA/Ag NCs to the G-quadruplex/hemin complex then leads to quenching of the fluorescence of the DNA/Ag NCs. To the best of our knowledge,

Scheme 1. (A) Schematic Illustration of PET between DNA/Ag NCs and the G-Quadruplex/Hemin Complex; (B) Comparison of the Redox State of the G-Quadruplex/Hemin Complex and the Energy Levels of DNA/Ag NCs; (C, D) Schematic Illustrations of the Analysis of DNA and ATP Using DNA/Ag NC−G-Quadruplex/Hemin Conjugates

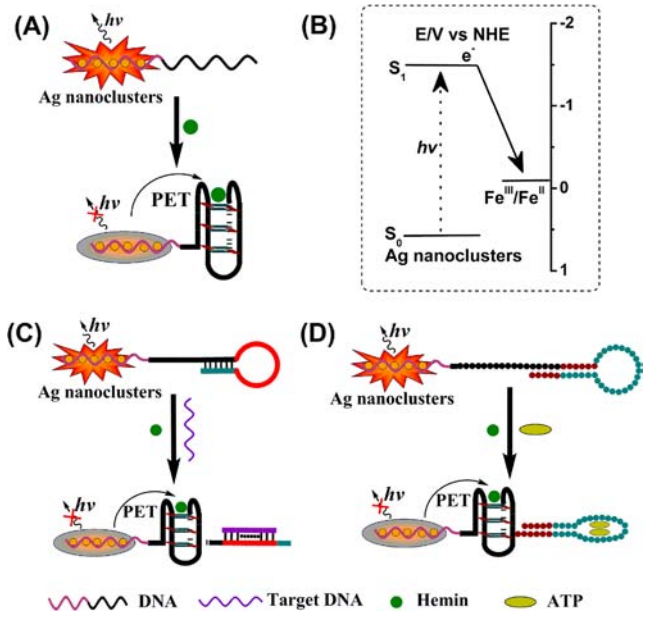

Received: September 10, 2012
Published: February 1, 2013

 © 2013 American Chemical Society dx.doi.org/10.1021/ja3089857 | J. Am. Chem. Soc. 2013, 135, 2403−2406

the present work is the first demonstration of the construction of a novel NMB based on in situ reduction and PET for use as a versatile biosensor.

To demonstrate such sensing concept, the fluorescent Ag nanoclusters were successfully prepared with strand A-G4 [Table S1 in the Supporting Information (SI)] as the synthesis template. Photographs of the Ag NCs under of room-light and UV irradiation are shown in the Figure 1A inset. A bright-red color

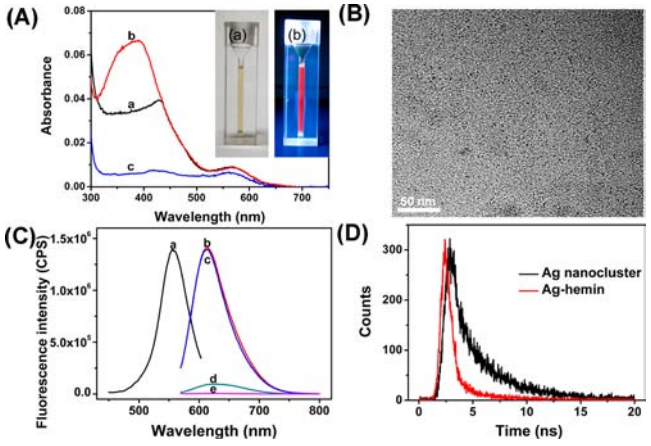

Figure 1. (A) UV−vis spectra of (a) DNA/Ag NCs, (b) DNA/Ag NCs in the presence of hemin, and (c) purified DNA/Ag NCs. The inset shows photographs of the Ag NCs under (a) room-light and (b) UV irradiation. (B) TEM image of DNA/Ag NCs. (C) (a) Excitation spectrum (λ_{max}^{ex} = 560 nm) and (b−d) emission spectra (λ_{max}^{em} = 620 nm) of DNA/Ag NCs obtained using strand A-G4 as the synthetic scaffold (b) alone, (c) in the presence of K^+, and (d) in the presence of K^+ and hemin. (e) Emission spectrum of DNA/Ag NCs obtained using strand G4 as the synthetic scaffold. (D) Fluorescence decay of DNA/Ag NCs in the (black) absence and (red) presence of hemin.

was observed under UV irradiation, indicating the formation of Ag NCs. The UV−vis absorption spectrum of the DNA/Ag NCs (Figure 1A, curve a) showed two peaks at 440 and 560 nm. Upon excitation at 560 nm, the DNA/Ag NCs showed a maximum emission at λ_{max}^{em} = 620 nm (Figure 1C, curve b). However, no fluorescence emission occurred upon excitation at 440 nm (Figure S1 in the SI, curve a). Although there were two peaks in the absorption spectrum, only the peak at 560 nm was the characteristic absorption of DNA/Ag NCs. After centrifugation of the DNA/Ag NCs, the peak at 440 nm almost disappeared (Figure 1A, curve c), and the absorbance at 560 nm also was slightly reduced (by 18%, as calculated from the absorbance intensity). The corresponding fluorescence spectrum (Figure S1, curve c) showed a decrease of ∼16.8%, consistent with the UV−vis results. Transmission electron microscopy (TEM) was also utilized to characterize the DNA/Ag NCs (Figure 1B and Figure S2). The product contained a lot of Ag NCs with an average diameter of 1.14 ± 0.43 nm and a small number of Ag nanoparticles (NPs), in accordance with the UV−vis spectroscopy results.

Upon excitation at the maximal absorption wavelength, the formed DNA/Ag NCs showed strong fluorescence intensity (Figure 1C, curve b) that was even slightly higher than the fluorescence intensity of DNA/Ag NCs after centrifugation, indicating that the small number of Ag NPs in the product had little impact on the fluorescence behavior of the Ag NCs (Figure S1). In the presence of K^+, the G-rich DNA sequence folded into a G-quadruplex structure stabilized by K^+, and the conformational change did not influence the fluorescence of the DNA/Ag NCs (Figure 1C, curve c). However, >93% quenching was observed for DNA/Ag NCs in the presence of both hemin and K^+ (Figure 1C, curve d). We also investigated the fluorescence intensity of DNA/Ag NCs at different concentrations of hemin and found that it decreased with increasing hemin concentration (Figure S3). Control experiments revealed that the interaction between hemin and the oligonucleotide without the G-quadruplex sequence (strand A-R; Table S1) and that between the G-quadruplex and the hemin derivative protoporphyrin IX (PPIX) did not lead to quenching of the fluorescence of the DNA/Ag NCs (Figure S4). Therefore, we can exclude the effects of potential nonspecific binding of hemin with the oligonucleotide and a change in the binding site of DNA/Ag NCs induced by the combination of hemin and the G-quadruplex. This strongly suggests that the fluorescence quenching resulted from the formation of the G-quadruplex/hemin complex, which placed hemin in close proximity to the DNA/Ag NCs.

As for the quenching mechanism, in theory, fluorescence quenching in this system could occur by collisional quenching, the formation of a nonfluorescent ground-state complex, energy transfer, or electron transfer. Here, several observations proved that PET occurs in this quenching process: (1) The absorption of the G-quadruplex/hemin complex (Figure 1A, curve b) is located at ∼400 nm, which does not overlap with the emission spectrum of DNA/Ag NCs (λ_{max}^{em} = 620 nm). Thus, fluorescence resonance energy transfer (FRET) from the DNA/Ag NCs to the G-quadruplex/hemin complex could be ruled out. (2) Hemin could not quench the fluorescence of DNA/Ag NCs under the same conditions, indicating that collisional quenching caused by hemin was not responsible for the present fluorescence quenching of the DNA/Ag NCs. (3) The absorption of the DNA/Ag NCs did not change in the presence of hemin, indicating that the decrease in fluorescence intensity was not induced by the change in the excitation wavelength, thereby eliminating static quenching upon formation of the ground-state complex as a possible mechanism. (4) Lifetime measurements were used to explore the quenching mechanism of the system. The fluorescence decay dynamics of the DNA/Ag NCs in the absence and presence of hemin are shown in Figure 1D. The fluorescence decay of the DNA/Ag NCs could be fitted using a monoexponential function with a time constant of 2.18 ± 0.02 ns, while in the presence of hemin, the fluorescence decay could be fitted using a dominant faster component with time constant of 0.769 ± 0.006 ns. Furthermore, the lifetimes of the DNA/Ag NCs were found to decrease with increasing hemin concentration (Figure S5). From these results, it can be concluded that the DNA/Ag NCs exhibited a significantly shorter fluorescence lifetime in the presence of hemin, presumably as a result of PET,[7] where the photoexcited electrons were transferred to the hemin (i.e., Fe^{III}−PPIX) complex. (5) The oxidation potential of purified DNA/Ag NCs was measured to be 0.351 V vs Ag/AgCl(saturated KCl) [0.573 V vs normal hydrogen electrode (NHE)] (Figure S6A, curve a), which is consistent with the previously reported result[4i] and different from that of the separated Ag NPs (0.467 V vs Ag/AgCl; Figure S6A, curve b). The hemin complex exhibited a quasi-reversible redox wave at a reduction potential of −0.383 V vs Ag/AgCl (−0.161 V vs NHE), corresponding to the Fe^{III}/Fe^{II}−PPIX couple (Figure S6B). On the basis of the above potential test results, a comparison of the redox state of the G-quadruplex/hemin complex and the energy levels of the DNA/Ag NCs (Scheme 1B) implies that the excited electrons of the DNA/Ag NCs can be transferred to the hemin complex. In

dx.doi.org/10.1021/ja3089857 | J. Am. Chem. Soc. 2013, 135, 2403−2406

addition, we note that similar mechanisms have been proposed in the literature for hemin at TiO_2 interfaces as well as CdSe/ZnS quantum dots (QDs).[8]

Interestingly, the PET effect was highly sensitive to the distance between the DNA/Ag NCs and the G-quadruplex/hemin complex and the structure of the DNA matrix. As shown in Figure S7, the quenching efficiency decreased with increasing distance. In addition, when the experiment was carried out in the presence of Pb^{2+}, a significantly less efficient PET process compared with that induced by K^+ was observed (Figure S8). This difference should be due to the relatively weak ability of the antiparallel G-quadruplex induced by Pb^{2+} to combine with hemin.[9] This result strongly suggests that the parallel G-quadruplex structure provides a more favorable template for PET than the antiparallel G-quadruplex structure. Since the efficiency of electron transport (ET) in DNA is dependent on the structure of the pathways that mediate ET through π-stacking base pairs,[10] it is conceivable that a G-quadruplex structure with π-stacked G-quartets and an ion channel in its center would favor DNA ET to a great extent.

The above results inspired us to use this novel system based on PET between DNA/Ag NCs and G-quadruplex/hemin to develop a new sensing platform for the detection of multiple targets. The analysis of DNA by the DNA/Ag NC−G-quadruplex/hemin system is depicted schematically in Scheme 1C. The oligonucleotide (A-G4-P1) used to form the DNA/Ag NCs includes a single-stranded loop complementary to the target DNA (red) along with the G-quadruplex sequence (black). A part of the G-quadruplex sequence forms a stable duplex domain in the stem region of the hairpin, caging the G-quadruplex sequence into a protected inactive configuration that eliminates the formation of the active G-quadruplex/hemin structure. Hybridization of the target DNA with the single-stranded loop opens the hairpin structure and releases the caged G-quadruplex sequence, allowing self-assembly of the G-quadruplex/hemin complex, which results in the quenching of the fluorescence of the DNA/Ag NCs.

Figure 2A shows the excitation spectrum (curve a) and emission spectrum (curve b) of the fluorescent Ag NCs obtained using strand A-G4-P1 as the synthetic scaffold. A shift in λ_{max}^{em} relative to that in Figure 1C was observed, which should be attributed to the change in the microenvironment of the DNA/Ag NCs. The formed DNA/Ag NCs showed strong fluorescence intensity. After the introduction of only hemin (curve c) or target DNA (curve d), there was almost no change in the fluorescence emission of the DNA/Ag NCs, indicating that the presence of either of them alone could not influence the fluorescence intensity. However, upon addition of both, the fluorescence intensity decreased sharply (curve e). This result indicates that the target DNA could combine with the loop of the hairpin structure, allowing the G-quadruplex/hemin complex to form, which resulted in a decrease in the fluorescence intensity. Figure 2B shows the fluorescence emission spectra of DNA/Ag NC−G-quadruplex/hemin hybrids in the presence of different concentrations of target DNA T1 (Table S1). As the concentration of T1 increased, the fluorescence intensity obviously decreased. Figure 2C shows the relationship between the fluorescence intensity and the concentration of T1. A good linear range from 1.0 to 100 nM and a detection limit of 0.6 nM could be obtained (Figure 2C inset), making this the most sensitive DNA sensor based on DNA/Ag NCs;[5a−c,6] its sensitivity is much better than or comparable to those of fluorescent dye- or QD-based sensing approaches.[11] To test the

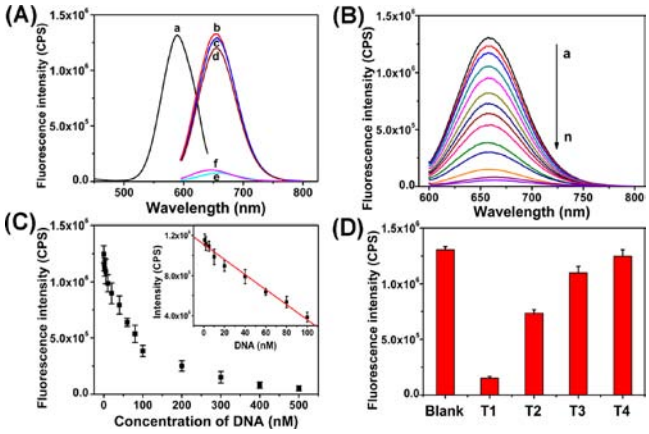

Figure 2. (A) (a) Excitation spectrum (λ_{max}^{ex} = 585 nm) and (b−e) emission spectra (λ_{max}^{em} = 655 nm) of DNA/Ag NCs obtained using strand A-G4-P1 as the synthetic scaffold (b) alone and (c−e) in the presence of (c) hemin, (d) target DNA, and (e) target DNA and hemin. (f) Emission spectrum of DNA/Ag NCs obtained using strand G4-P1 as the synthetic scaffold. (B) Fluorescence emission spectra at different T1 concentrations (0, 1, 2, 5, 10, 20, 40, 60, 80, 100, 200, 300, 400, and 500 nM from a to n). (C) Relationship between the fluorescence intensity and the concentration of T1. The inset shows the linear relationship over the concentration range from 1 to 100 nM. (D) Selectivity of target DNA analysis.

specificity of this sensing system, other DNA strands with one (T2), two (T3), and four (T4) mismatched nucleotides (Table S1) were also investigated. Figure 2D shows the fluorescence changes for the target DNA and the mismatched DNA strands. These results clearly demonstrate that the detection approach shows a high selectivity toward the target DNA, allowing even one mismatched nucleotide to be distinguished.

To demonstrate further the feasibility and universality of present proof-of-concept, a homogeneous model was adopted for detection of adenosine triphosphate (ATP) with just a little change in the sensing sequence. As shown in Scheme 1D, the oligonucleotide A-G4-ATP (Table S1) assembles into a hairpin structure consisting of the G-quadruplex sequence (black) and the aptamer sequence against ATP (blue). This hairpin composition ensures that parts of the aptamer and G-quadruplex sequences are caged in the duplex structure of the stem of the hairpin. Formation of the ATP−aptamer complex opens the hairpin structure and deprotects the G-quadruplex sequence, and self-assembly of the G-quadruplex/hemin complex leads to quenching of the fluorescence of the DNA/Ag NCs.

The feasibility of the experimental principle was examined under different conditions. From the results shown in Figure 3A, we could conclude that the ATP indeed combined with the loop of the hairpin structure and induced the formation of the G-quadruplex/hemin complex, resulting in a decrease in the fluorescence intensity. We further explored the fluorescence emission spectra of the DNA/Ag NC−G-quadruplex/hemin interaction in the presence of different concentrations of ATP (Figure 3B). The results showed that as the ATP concentration increased, the fluorescence intensity decreased accordingly. Figure 3C shows the relationship between the fluorescence intensity and the ATP concentration, and the inset shows the calibration curve for quantitative analysis of ATP. The intensity was linearly dependent on the concentration of ATP over the range from 0.02 to 1.0 μM ($|R|$ = 0.990), and the detection limit was found to be 8.0 nM based on the signal-to-noise ratio; this is

dx.doi.org/10.1021/ja3089857 | J. Am. Chem. Soc. 2013, 135, 2403−2406

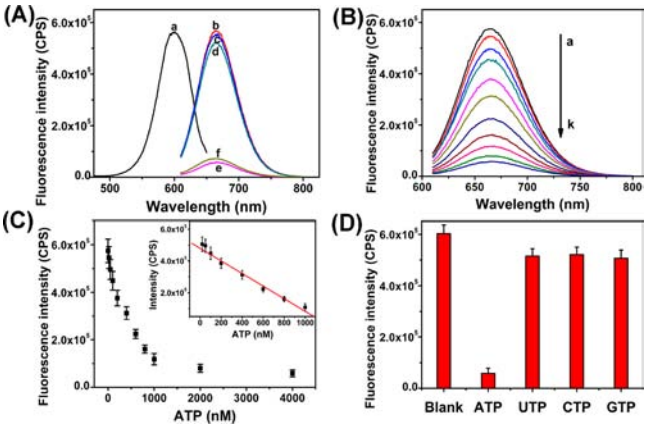

Figure 3. (A) (a) Excitation spectrum (λ_{max}^{ex} = 600 nm) and (b–e) emission spectra (λ_{max}^{em} = 665 nm) of Ag NCs obtained using strand A-G4-ATP as the synthetic scaffold (b) alone and (c–e) in the presence of (c) hemin, (d) ATP, and (e) ATP and hemin. (f) Emission spectrum of Ag NCs obtained using strand G4-ATP as the synthetic scaffold. (B) Fluorescence emission spectra at different ATP concentrations (0, 0.02, 0.05, 0.1, 0.2, 0.4, 0.6, 0.8, 1.0, 2.0, and 4.0 μM from a to k). (C) Relationship between the fluorescence intensity and the ATP concentration. The inset shows over the concentration range from 0.02 to 1.0 μM. (D) Selectivity of ATP analysis.

lower than or comparable to the detection limits for most of the previously reported fluorescent aptasensors for ATP detection.[5g,12] Similarly, we demonstrated the selectivity of the aptamer sensor system using the ATP analogues GTP, CTP, and UTP (Figure 3D). It was found that ATP resulted in an obvious change in the fluorescence, while the fluorescence changes in the presence of the analogues were nearly negligible. These results demonstrate that this approach exhibits excellent selectivity for ATP detection over competing nucleoside triphosphates.

In conclusion, we have demonstrated a new system involving PET between DNA/Ag NCs and G-quadruplex/hemin complexes that can be used as an NMB for the sensitive and selective detection of DNA and ATP. Compared with conventional MBs, this NMB shows some unique features: (1) It is very simple and does not require separation and troublesome procedures. (2) It avoids complex labeling processes, as DNA/Ag NCs serve as the fluorescent probe and the G-quadruplex/hemin complex as the acceptor. (3) It can be used for multiple targets with only small changes in the sensing sequence. (4) It shows very low background fluorescence, which is beneficial for improving the sensitivity. More importantly, the photoluminescence emission band of the DNA/Ag NCs could be readily tuned by changing the oligonucleotide sequence. It is expected that multiplex NMBs could be potentially realized by designing multiple templates containing different functional domain sequences (generating fluorescent DNA/Ag NCs with different emission peaks). Therefore, the construction of this innovative NMB is vital to the development of analytical science. Furthermore, this study also provides a successful paradigm for exploring new and interesting properties of functional nanomaterials and thus extending their applications in multiple fields.

■ ASSOCIATED CONTENT

Ⓢ Supporting Information

DNA sequences, detailed experimental methods, and additional data. This material is available free of charge via the Internet at http://pubs.acs.org.

■ AUTHOR INFORMATION

Corresponding Author

ekwang@ciac.jl.cn

Notes

The authors declare no competing financial interest.

■ ACKNOWLEDGMENTS

The work was supported by the National Natural Science Foundation of China (21075120, 21190040) and the 973 Program (2010CB933600, 2011CB911000).

■ REFERENCES

(1) Tyagi, S.; Kramer, F. R. *Nat. Biotechnol.* **1996**, *14*, 303.

(2) (a) Bonnet, G.; Krichevsky, O.; Libchaber, A. *Proc. Natl. Acad. Sci. U.S.A.* **1998**, *95*, 8602. (b) Yang, C. Y. J.; Lin, H.; Tan, W. H. *J. Am. Chem. Soc.* **2005**, *127*, 12772. (c) Bonnet, G.; Tyagi, S.; Libchaber, A.; Kramer, F. R. *Proc. Natl. Acad. Sci. U.S.A.* **1999**, *96*, 6171.

(3) Tyagi, S.; Bratu, D. P.; Kramer, F. R. *Nat. Biotechnol.* **1998**, *16*, 49.

(4) (a) Peyser, L. A.; Vinson, A. E.; Bartko, A. P.; Dickson, R. M. *Science* **2001**, *291*, 103. (b) Zheng, J.; Dickson, R. M. *J. Am. Chem. Soc.* **2002**, *124*, 13982. (c) Yu, J.; Patel, S. A.; Dickson, R. M. *Angew. Chem., Int. Ed.* **2007**, *46*, 2028. (d) Latorre, A.; Somoza, A. *ChemBioChem* **2012**, *13*, 951. (e) Han, B.; Wang, E. *Anal. Bioanal. Chem.* **2012**, *402*, 129. (f) Zheng, J.; Nicovich, P. R.; Dickson, R. M. *Annu. Rev. Phys. Chem.* **2007**, *58*, 409. (g) Richards, C. I.; Choi, S.; Hsiang, J.-C.; Antoku, Y.; Vosch, T.; Bongiorno, A.; Tzeng, Y.-L.; Dickson, R. M. *J. Am. Chem. Soc.* **2008**, *130*, 5038. (h) Petty, J. T.; Story, S. P.; Juarez, S.; Votto, S. S.; Herbst, A. G.; Degtyareva, N. N.; Sengupta, B. *Anal. Chem.* **2012**, *84*, 356. (i) Sharma, J.; Rocha, R.; Phipps, M.; Yeh, H.; Balatsky, K.; Vu, D.; Shreve, A.; Werner, J.; Martinez, J. *Nanoscale* **2012**, *4*, 4107. (j) Vosch, T.; Antoku, Y.; Hsiang, J. C.; Richards, C. I.; Gonzalez, J. I.; Dickson, R. M. *Proc. Natl. Acad. Sci. U.S.A.* **2007**, *104*, 12616.

(5) (a) Yang, S. W.; Vosch, T. *Anal. Chem.* **2011**, *83*, 6935. (b) Yeh, H.-C.; Sharma, J.; Han, J. J.; Martinez, J. S.; Werner, J. H. *Nano Lett.* **2010**, *10*, 3106. (c) Lan, G.-Y.; Chen, W.-Y.; Chang, H.-T. *Biosens. Bioelectron.* **2011**, *26*, 2431. (d) Sharma, J.; Yeh, H.-C.; Yoo, H.; Werner, J. H.; Martinez, J. S. *Chem. Commun.* **2010**, *46*, 3280. (e) Sharma, J.; Yeh, H.-C.; Yoo, H.; Werner, J. H.; Martinez, J. S. *Chem. Commun.* **2011**, *47*, 2294. (f) Li, J.; Zhong, X.; Zhang, H.; Le, X. C.; Zhu, J. *Anal. Chem.* **2012**, *84*, 5170. (g) Zhou, Z.; Du, Y.; Dong, S. *Biosens. Bioelectron.* **2011**, *28*, 33.

(6) (a) Guo, W.; Yuan, J.; Dong, Q.; Wang, E. *J. Am. Chem. Soc.* **2010**, *132*, 932. (b) Yeh, H. C.; Sharma, J.; Shih, I. M.; Vu, D. M.; Mattinez, J. S.; Werner, J. H. *J. Am. Chem. Soc.* **2012**, *134*, 11550.

(7) Patel, S. A.; Cozzuol, M.; Hales, J. M.; Richards, C. I.; Sartin, M.; Hsiang, J.-C.; Vosch, T.; Perry, J. W.; Dickson, R. M. *J. Phys. Chem. C* **2009**, *113*, 20264.

(8) (a) Obare, S. O.; Ito, T.; Balfour, M. H.; Meyer, G. J. *Nano Lett.* **2003**, *3*, 1151. (b) Sharon, E.; Freeman, R.; Willner, I. *Anal. Chem.* **2010**, *82*, 7073.

(9) Li, T.; Wang, E.; Dong, S. *J. Am. Chem. Soc.* **2009**, *131*, 15082.

(10) Genereux, J. C.; Barton, J. K. *Chem. Rev.* **2010**, *110*, 1642.

(11) (a) Yang, R.; Tang, Z.; Yan, J.; Kang, H.; Kim, Y.; Zhu, Z.; Tan, W. *Anal. Chem.* **2008**, *80*, 7408. (b) Zhang, L.; Guo, S.; Dong, S.; Wang, E. *Anal. Chem.* **2012**, *84*, 3568. (c) Kim, J. H.; Chaudhary, S.; Ozkan, M. *Nanotechnology* **2007**, *18*, No. 195105. (d) Cady, N. C.; Strickland, A. D.; Batt, C. A. *Mol. Cell. Probes* **2007**, *21*, 116. (e) Freeman, R.; Liu, X.; Willner, I. *J. Am. Chem. Soc.* **2011**, *133*, 11597.

(12) (a) Lee, D.; Kim, S.; Hong, J. *Angew. Chem., Int. Ed.* **2004**, *43*, 4777. (b) Zhang, L.; Wei, H.; Li, J.; Li, T.; Li, D.; Li, Y.; Wang, E. *Biosens. Bioelectron.* **2010**, *25*, 1897. (c) Liu, X.; Freeman, R.; Willner, I. *Chem.—Eur. J.* **2012**, *18*, 2207. (d) Zhang, M.; Guo, S.; Li, Y.; Zuo, P.; Ye, B. *Chem. Commun.* **2012**, *48*, 5488.